# NUMERICAL CALCULATION OF BEAM COUPLING IMPEDANCES FOR THE SIS-100 SYNCHROTRON FOR FAIR*

U. Niedermayer# and O. Boine-Frankenheim
Technische Universität Darmstadt, Institut für Theorie Elektromagnetischer Felder (TEMF),
Schlossgartenstraße 8, 64289 Darmstadt, Germany

*Abstract*

The transverse impedance of kicker magnets is considered to be one of the main beam instability sources in the projected SIS-100 at FAIR and also in the SPS at CERN. The longitudinal impedance can contribute to the heat load, which is especially a concern in the cold sections of SIS-100. In the high frequency range, time domain codes are commercially available to calculate the impedance but they become inapplicable at medium and low frequencies. We present the ongoing work of developing a Finite Integration (FIT) solver in frequency domain which is based on the Parallel and Extensible Toolkit for Scientific computing (PETSc) framework in C++. The code is applied to an inductive insert used to compensate the longitudinal space charge impedance in low energy machines. Another application focuses on the transverse impedance contribution of a ferrite kicker with inductively coupled pulse forming network (PFN) and frequency dependent complex material permeability. In future we plan to confirm our simulations with dedicated wire or coil bench measurements.

## INTRODUCTION

For the SIS100 synchrotron which will be built in the framework of the FAIR project, especially the coasting beam and the high intensity proton bunch are susceptible to impedance driven coherent transverse instabilities. Since SIS100 will contain ferrite kickers in cryogenic ($< 20$ K) sections, the beam induced heat load (as also recently reported on LHC-kickers) is an important issue. In the relevant frequency range of several kHz up to the beam pipe cutoff, impedance sources are mainly given by the thin stainless steel beam pipe [1] and ferrite components. Broadband cavities dominate the longitudinal impedance [2]. Slightly below the cutoff frequency, cross-section changes such as collimators might have an impact. Additionally to the necessary ferrite kickers and their supply networks, also an inductive ferrite insertion to compensate the negative inductive longitudinal space charge impedance has been proposed. We will focus on this insert which serves as a test case for the code discussed in this paper. Nonetheless, the main application of the code will be the transverse impedance of SIS100 kicker modules.

Usually coupling impedances are defined as the Fourier transform of the wake function which can be calculated by time domain (TD) codes such as CST Particle Studio [3]. At low frequencies, which become more important for large hadron synchrotrons, this technique is inapplicable due to the necessary large wake length (frequency resolution limitation by Küpfmüller's uncertainty principle [4]).

The following will give a definition of the coupling impedances directly in frequency domain (FD). Underlined symbols emphasize complex variables. This also serves to distinguish between TD and FD. The beam with total charge $q$ in a synchrotron is modeled as a disc with radius $a$ of uniform surface charge density $\sigma$ traveling with velocity $v$. The transverse displacement $d_x$ of the beam (i.e. a coherent dipole oscillation) is approximated to first order by

$$\sigma(\varrho,\varphi) \approx \frac{q}{\pi a^2}\left[\Theta(a-\varrho)+\delta(a-\varrho)d_x\cos\varphi\right] \quad (1)$$

where $\Theta$ is the unit step and $\delta$ is its generalized derivative. The beam current density in frequency domain is

$$\underline{J}_{s,z}(\varrho,\varphi,z;\omega) = \int_{-\infty}^{\infty} v\sigma(\varrho,\varphi)\delta(z-vt)e^{-i\omega t}\mathrm{d}t \quad (2)$$

$$= \sigma(\varrho,\varphi)e^{-i\omega z/v} =: \underline{J}_{\parallel} + \underline{J}_{\perp} \quad (3)$$

where $\underline{J}_{\parallel}$ and $\underline{J}_{\perp}$ are the monopole and dipole components, as in Eq. (1), respectively. The coherent force due to beam induced electromagnetic fields acting back on the beam is described by the coupling impedance [5]

$$\underline{Z}_{\parallel}(\omega) = -\frac{1}{q^2}\int_{\mathrm{beam}} \underline{\vec{E}}\cdot\underline{\vec{J}}_{\parallel}^{\,*}\,\mathrm{d}V \quad (4)$$

$$\underline{Z}_{\perp,x}(\omega) = -\frac{v}{(qd_x)^2\omega}\int_{\mathrm{beam}} \underline{\vec{E}}\cdot\underline{\vec{J}}_{\perp}^{\,*}\mathrm{d}V. \quad (5)$$

The electric field $\underline{\vec{E}}$ is to be calculated from Maxwell's equations. Instead of the cosine distribution for dipolar excitation in Eq. (1) one can also use a twin wire approximation, as described in [6].

## INDUCTIVE INSERT

The longitudinal space charge impedance [7]

$$\underline{Z}_{\parallel}^{SC}(\omega,\beta) = -i\omega\frac{\mu_0 g l}{4\pi\beta^2\gamma^2} \quad (6)$$

constitutes a major fraction of the imaginary part of the longitudinal impedance in SIS100. This leads to a RF-potential-well distortion and to a net decrease of the RF-voltage (decrease of bucket height). We will discuss a tubu-

* Work supported by GSI
# u.niedermayer@gsi.de



ISBN 978-3-95450-118-2

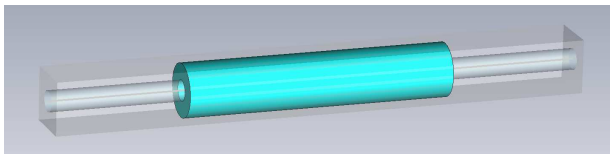

Figure 1: Tubular ferrite ($\underline{\mu} = \underline{\mu}_r\mu_0$ , $\underline{\mu}_r = \mu_r' - i\mu_r''$) insert with radii $a = 40$ mm, $b = 100$ mm and length $l = 1$ m in perfectly conducting (PEC) background.

lar inductive insert (see Fig. 1) which is supposed to compensate the negative inductance described by Eq. (6). Different 2D analytical simplifications with either beam radius equal tube inner radius (validity see [8]) or pencil beam are considered.

### *Magneto-Statics*

In this most simplified case the beam is considered as constant DC current. One obtains from the flux to current ratio

$$\underline{Z}_{\parallel}^{\mathrm{MS}}(\omega) = i\omega L = i\omega\frac{\underline{\mu} l}{2\pi}\ln(b/a) \tag{7}$$

independent of the beam's velocity.

### *Magneto-Quasi-Statics*

The standard formalism to calculate the longitudinal space charge impedance [7] is generalized to ferrite pipes. With $g_0 = 1 + 2\log(b/a)$ and $\underline{g}_r = (1 + 2\underline{\mu}_r \log(b/a))/g_0$ one obtains

$$\underline{Z}_{\parallel}^{\mathrm{MQS}}(\omega,\beta) = -i\omega\frac{\mu_0 g_0 l}{4\pi\beta^2}\left(1 - \underline{g}_r + \frac{\underline{g}_r}{\gamma^2}\right). \tag{8}$$

which reduces to the well known SC impedance Eq. (6) for $\underline{\mu} = \mu_0$. For simplicity, the vacuum layer between beam and ferrite has been omitted.

### *Fullwave Calculation*

For the fullwave calculation the fields are split into source [5]

$$\underline{E}_z^S(\varrho,\omega) = iq\frac{\mu_0}{2\pi}\frac{\omega}{\beta^2\gamma^2}\mathrm{K}_0(\mathrm{k}_\varrho^{\mathrm{vac}}\varrho) \tag{9}$$

$$\underline{H}_\varphi^S(\varrho,\omega) = q\frac{1}{2\pi c_0}\frac{\omega}{\beta\gamma}\mathrm{K}_1(\mathrm{k}_\varrho^{\mathrm{vac}}\varrho) \tag{10}$$

and scattered (decelerating) parts

$$\underline{E}_z^{\mathrm{dec}}(\varrho,\omega) = A\mathrm{J}_0(\mathrm{k}_\varrho^{\mathrm{vac}}\varrho) \tag{11}$$

in vacuum with $k_\varrho^{\mathrm{vac}} = \omega/(\beta\gamma c)$. In ferrite one has

$$k_\varrho^{\mathrm{f}} = k_\varrho^{\mathrm{vac}}\sqrt{(\underline{\mu}_r - 1)\beta^2\gamma^2 - 1} \tag{12}$$

and the fields are

$$\underline{E}_z^{\mathrm{f}}(\varrho,\omega) = B\left(\mathrm{H}_0^{(1)}(\mathrm{k}_\varrho^{\mathrm{f}}\varrho) - \frac{\mathrm{H}_0^{(1)}(\mathrm{k}_\varrho^{\mathrm{f}}\mathrm{b})}{\mathrm{H}_0^{(2)}(\mathrm{k}_\varrho^{\mathrm{f}}\mathrm{b})}\mathrm{H}_0^{(2)}(\mathrm{k}_\varrho^{\mathrm{f}}\varrho)\right)$$

$$\underline{H}_\varphi^{\mathrm{f}}(\varrho,\omega) = \frac{1}{i\omega\mu_0(\underline{\mu}_r - \beta^{-2})}\partial_\varrho\underline{E}_z^{\mathrm{f}}(\varrho,\omega). \tag{13}$$

These equations can be solved for $A$ and $B$ by matching the fields at the ferrite boundary as

$$\underline{E}_z^S(a,\omega) + \underline{E}_z^{\mathrm{dec}}(a,\omega) = \underline{E}_z^{\mathrm{f}}(a,\omega) \tag{14}$$

$$\underline{H}_\varphi^S(a,\omega) = \underline{H}_\varphi^{\mathrm{f}}(a,\omega) \tag{15}$$

The solution is obtained symbolically by Mathematica [9] and displayed in Fig 3. Note that only the MQS approach includes the negligibly small part of the beam's space charge impedance within the insert.

## NUMERICAL APPROACH IN FD

In this section we briefly describe our numerical approach to impedance calculation using the Finite Integration Technique(FIT). The monopolar excitation current is given as a discretization of (3) with constant $\sigma$ as

$$\underline{\widehat{\mathbf{j}}}_{e,z}^{\mathrm{mono}}(i_z) = \int_{\tilde{A}_z}\underline{\vec{J}}\cdot\mathrm{d}\vec{A} = qe^{-i\omega z_i/v} \tag{16}$$

where $i_z$ is the $z$-index and $z_i$ is its $z$ coordinate. The dipolar excitation current is modeled by the twin wire dipole approximation as

$$\underline{\widehat{\mathbf{j}}}_{e,z}^{\mathrm{dip}}(i_z) = \underline{\widehat{\mathbf{j}}}_{e,z}^{\mathrm{mono}}(x = -d_x) - \underline{\widehat{\mathbf{j}}}_{e,z}^{\mathrm{mono}}(x = +d_x). \tag{17}$$

From the discrete Maxwell equations one obtains the wave equation (see [10] and references therein)

$$\left(\widetilde{\mathbf{C}}\mathbf{M}_{\mu^{-1}}\mathbf{C} + i\omega\mathbf{M}_\kappa - \omega^2\mathbf{M}_\varepsilon\right)\underline{\widehat{\mathbf{e}}} = -i\omega\underline{\widehat{\mathbf{j}}}_e \tag{18}$$

subject to PEC boundary conditions in $x$ and $y$ direction and phase corrected periodic boundary conditions (see [10]) in $z$ direction. Note that the beam's charge is implicitly included by the continuity equation. First, the system is symmetrically rewritten with $\underline{\widehat{\mathbf{e}}} = \mathbf{M}_\varepsilon^{-1/2}\underline{\widehat{\mathbf{e}}}'$ as

$$(\mathbf{M}_\varepsilon^{-1/2}\widetilde{\mathbf{C}}\mathbf{M}_{\mu^{-1}}\mathbf{C}\mathbf{M}_\varepsilon^{-1/2} + i\omega\mathbf{M}_\varepsilon^{-1}\mathbf{M}_\kappa - \omega^2 I)\underline{\widehat{\mathbf{e}}}' = -i\omega\mathbf{M}_\varepsilon^{-1/2}\underline{\widehat{\mathbf{j}}}_e \tag{19}$$

which we will abbreviate by $\mathbf{A}\underline{\widehat{\mathbf{e}}}' = b$. For easier numerical treatment a Helmholtz split $\underline{\widehat{\mathbf{e}}} = \underline{\widehat{\mathbf{e}}}_g + \underline{\widehat{\mathbf{e}}}_c$ with $\mathbf{C}\underline{\widehat{\mathbf{e}}}_g = 0$ and $\mathbf{S}\underline{\widehat{\mathbf{e}}}_c = 0$ (see also[11]) is performed. The static part of the field is solved by Poisson's equation

$$\widetilde{\mathbf{S}}\mathbf{M}_\varepsilon\widetilde{\mathbf{S}}^H\underline{\Phi} = \frac{i}{\omega}\widetilde{\mathbf{S}}\underline{\widehat{\mathbf{j}}}_e, \qquad \underline{\widehat{\mathbf{e}}}_g = -\widetilde{\mathbf{S}}^H\underline{\Phi} \tag{20}$$

where the right hand side is the charge in dual volumes obtained by the continuity equation. Equation (19) reads then

$$\mathbf{A}\underline{\widehat{\mathbf{e}}}_c' = -i\omega\mathbf{M}_\varepsilon^{-1/2}\underline{\widehat{\mathbf{j}}}_e + \omega^2\mathbf{M}_\varepsilon^{1/2}\underline{\widehat{\mathbf{e}}}_g \tag{21}$$

with a divergence-free right hand side. This split reduces the iterations of PETSc's SSOR preconditioned GMRES solver [12] tremendously while the cost for solving Eq. (20) is negligibly small. The integral in the impedance definitions in Eqs. (4) and (5) is evaluated by the functional

$$Z(\underline{\widehat{\mathbf{e}}}(\omega)) = \underline{\widehat{\mathbf{e}}}\cdot\underline{\widehat{\mathbf{j}}}_e^* \tag{22}$$

with normalized magnitude of the current ($q = 1$ As).

ISBN 978-3-95450-118-2

*Software*

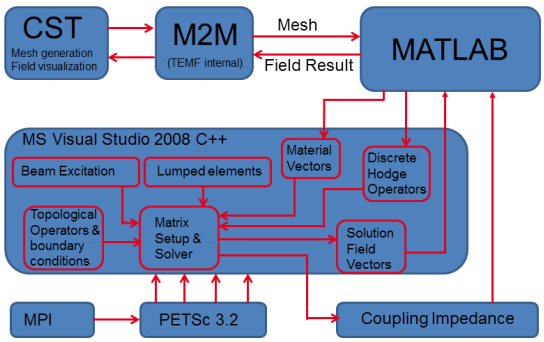


Figure 2: Implementation

The CAD constructions and the mesh originate from CST EMS2011 [3]. It is imported via Matlab [13] where the material operators are disassembled in order to obtain the staircase material vectors. This allows to rescale the material parameters frequency dependently within the main program. Mesh data, material vectors and topological (PEC) information are transferred to the C++ main program. The actual high performance computations are carried out by the PETSc 3.2 [12] package which provides a variety of matrix structures, preconditioners and solvers for either real or complex linear systems. After computation, the fields can be visualized by transferring results back to Matlab and CST EMS2011 (see Fig. 2).

## PRELIMINARY RESULTS

A comparison between the different analytical and numerical approaches can be seen in Fig. 3. For simplicity, $\underline{\mu}_r = 1000 - 100i$ was chosen independent of the frequency such that structural properties become better visible. As desired, the low frequency part of the insert impedance can compensate the space charge impedance of the whole ring.

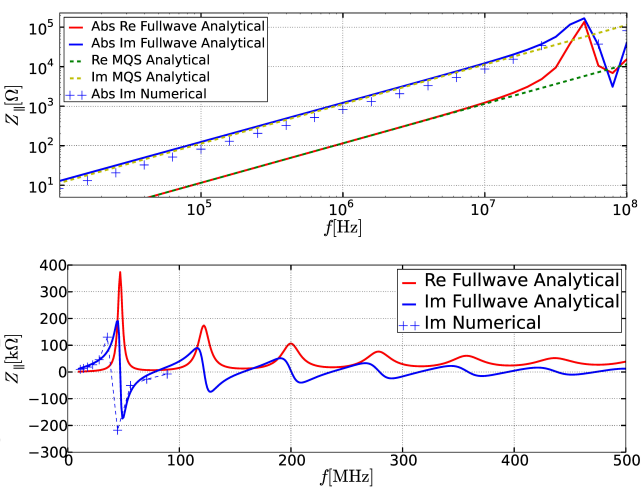


Figure 3: Longitudinal impedance for the inductive insert in Fig. 1 for $\beta = 0.3$. The resonances inaccurately displayed in the upper plot are enlarged in the lower one.

As a rule of thumb one should think factor 1000 shorter than the ring and factor 1000 higher permeability than vacuum compensates. Nonetheless, a ruinous disadvantage are resonances which occur at higher frequencies (see lower part of Fig. 3). These resonances, together with the real part of $\underline{\mu}_r$ cause a very high real part of $\underline{Z}_\parallel$ triggering the 'microwave instability' (see also [14]).

The rather poor accuracy of the numerical calculation originates mainly from insufficient mesh resolution (7000 staircase cells). Note also that the 3D numerical calculation contains finite length effects which are not represented in the analytical models. The numerical calculation of the real part will be presented in the near future.

## CURRENT STATUS AND OUTLOOK

The current status of our code is that without ferrite material up to $10^6$ mesh cells can be simulated. The high permeability of ferrite deteriorates the condition number of the system matrix tremendously such that iterative solvers do not always converge. In this case for small number of mesh cells direct solvers can be employed. In future we will address the transverse impedance of SIS-100 kickers. Besides the ferrite itself, also the kicker pulse forming network (PFN) contributes to the dipolar impedance. Its frequency dependent impedance [15] will be included as lumped element in the simulation. For the confirmation of the obtained results, bench measurements are outlined.

## REFERENCES

[1] U. Niedermayer and O. Boine-Frankenheim, Analytical and numerical calculations of resistive wall impedances for thin beam pipe structures at low frequencies, NIM A 687, 2012.

[2] P. Spiller et al., FAIR TDR SIS100, 2008.

[3] CST Studio Suite®, www.cst.com

[4] K. Küpfmüller, Einführung in die theoretische Elektrotechnik, Springer, 1932.

[5] R. Gluckstern, CAS, 2000.

[6] G. Nassibian and F. Sacherer, Methods for measuring transverse coupling impedances in circular accelerators, NIM, 1979.

[7] K. Schindl, CAS, 2000.

[8] A. Al-Khateeb et al., Comparison of the longitudinal coupling impedance from different source terms, NIM A, 2008.

[9] Mathematica®, www.wolfram.com/mathematica

[10] U. Niedermayer and O. Boine-Frankenheim, Numerical Calculation of Beam Coupling Impedances in the Frequency Domain using FIT, Proc. of ICAP, 2012.

[11] B. Doliwa and T. Weiland, Numerical Computation of Kicker Impedances: Towards a complete Database for the GSI SIS100/300 Kickers, Proc. of ICAP, 2006.

[12] PETSc, www.mcs.anl.gov/petsc

[13] Matlab®, www.mathworks.de

[14] C. Beltran, PhD thesis, 2003.

[15] K. Samuelsson et al., Proc. of IPAC, 2011.



ISBN 978-3-95450-118-2